RSC Advances

PAPER

View Article Online
View Journal | View Issue

Cite this: *RSC Adv.*, 2025, **15**, 47315

Computational design and exploitation of bulk and surface molecularly imprinted polymers for removal of simmondsin from *Simmondsia chinensis* residual seeds

Sara T. Elmahdy,[ab] Ali M. El-Halawany,[c] Hussein M. Fahmy[a] and Rasha M. El Nashar *[a]

Herein, we report for the first time the application of molecularly imprinted polymer (MIP) for the extraction of simmondsin (SIMM) from *Simmondsia chinensis* residual seeds (jojoba meal). A computational study was conducted to determine the optimal template-to-functional monomer molar ratio for MIP preparation. Based on this, MIPs were synthesized *via* a non-covalent approach employing itaconic acid (ITC) as a functional monomer, in bulk and surface imprinting techniques. Batch rebinding experiments revealed that surface-imprinted polymer at a 1 : 4 : 40 molar ratio, with higher binding efficiency compared to the bulk-synthesized MIPS. This MIP exhibited selective binding ability towards simmondsin in the presence of structural analogues, achieving a simmondsin removal rate of 92.46% ± 0.02 from jojoba meal extract and keeping the protein content at a higher value of 25.88% ± 0.72% which is comparable to the estimated range of 26–33% before extraction, thus, preserving its nutritional value for potential use as animal feed.

Received 23rd October 2025
Accepted 17th November 2025

DOI: 10.1039/d5ra08130k

rsc.li/rsc-advances

1. Introduction

The Jojoba plant (*Simmondsia chinensis*), a member of the Simmondsiaceae family, is a botanical marvel renowned for its adaptability and ability to live for many years, and grows well in dry places like deserts and commercial significance. This special bush, can survive where other plants cannot, and is reported to grow in countries like the United States, Argentina, Chile, India, Tunisia, and Egypt.[1] The jojoba seed is the most valuable part of the plant; nearly half of its content is present as a liquid wax known as jojoba oil. This unique oil finds applications in diverse industries including: cosmetics, pharmaceuticals, lubricants, and even petrochemicals. Furthermore, its properties make it suitable for biodiesel production and fuel enhancement.[2–4] On another level, this golden oil is used in the medical field, where it is used as an antimicrobial, antifungal, and anti-inflammatory.[1]

The residual material derived from jojoba seeds following oil extraction, commonly referred to as jojoba seed meal, presents a compelling prospect as a nutritional supplement for animals. This is primarily attributed to its substantial protein content, ranging from 26 to 33%, which is essential for animal growth and development. However, a formidable obstacle impedes the full realization of jojoba meal's potential as a livestock feed, relying on the presence of a significant concentration of toxic glycosides constituting approximating 15 percent of the meal's composition, which poses a substantial risk to animal health.

Compounds such as simmondsin and simmondsin-2-ferulate have been identified as the primary toxic glycosides responsible of the reported adverse effects, specially simmondsin [5,6] due to its detrimental impact on animal well-being by diminishing feed consumption, stunting growth, compromising reproductive capacity, and disrupting vital biochemical processes within the animal's system.[7,8] On the other hand, simmondsin was reported to be potent anti-obesity agent, where a dose of around 0.15–0.25% level significantly reduced food intake and body weight without apparent negative effects or hepatotoxicity, which indicates possibility of its application after regulating the up taken dose.[9–11]

Various chemical, biological, and enzymatic approaches were explored to eliminate simmondsin and simmondsin-2-ferulate from jojoba seed meal.[7] Chemical extraction of simmondsin and its derivatives was performed by soaking the meal in boiling water and different solvents such as methanol, ethanol, isopropanol, butanol, and acetone. With high removal percentages, especially boiling water and 80% ethanol removes almost 95% of simmondsin, and isopropanol removes 83%of simmondsin content[12–14]

Also, ammonia and hydrogen peroxide as degradation materials aim to inactivate or degrade simmondsin rather than

[a]*Chemistry Department, Faculty of Science, Cairo University, Giza, 12613, Egypt. E-mail: rasha.elnashar@cu.edu.eg; rashaelnashar@gmail.com*
[b]*Nawah Scientific, Al-Asmarat, Almokattam Mall, Street 9, Cairo, Egypt*
[c]*Pharmacognosy Department, Faculty of Pharmacy, Cairo University, Giza, Egypt*

purely extract it chemically.[13] Despite that, these methods were found to be effective for the removal of simmondsin and its derivatives they were reported to have a negative impact on the protein and carbohydrate content rendering the resulting meal to have no nutritional value.

Alternative approaches, such as biological and enzymatic treatments, have emerged as environmentally preferable options for detoxifying jojoba meal. Biological treatments primarily involve the use of microorganisms (bacteria, fungi) to degrade or metabolize simmondsin into non-toxic compounds. These methods leverage the metabolic pathways of the microbes. For example, fermentation with different strains of lactic acid bacteria like *Lactobacillus acidophilus*, *Bifidobacterium angulatumand*, and *Streptococcus thermophiles* has shown to be promising in reducing simmondsin levels *via* breaking down the simmondsin molecules, converting them into less toxic or non-toxic derivatives.[7,15,16] While biological and enzymatic treatments generally preserve a higher proportion of protein and carbohydrates compared to their chemical counterparts, they are associated with significantly elevated operational costs, besides their economic implications and operational limitations that largely hindered their widespread adoption.[2,7]

Molecularly imprinted polymers (MIP) represent a promising class of synthetic polymers that can be engineered to possess specific recognition sites that are complementary in shape, size, and chemical functionality to a target molecule, acting much like a lock and key,[17] accordingly, they were reported to have several applications like chemical and biological sensing, where MIPs serve as robust recognition elements in sensors, natural receptors like antibodies, and are widely used in biosensors for detecting specific biological molecules, environmental pollutants, or hazardous substances, with recent advancements including their integration with smartphone technology for portable, on-site analysis, enabling rapid detection of targets like pesticide residues.[18–20]

MIPs can also be employed as intelligent drug carriers capable of releasing therapeutic agents in response to specific stimuli (*e.g.*, pH, temperature, or light), which allows for controlled and sustained drug release; MIPs can be utilized in diagnostic tests for detecting biomarkers related to diseases such as cancer, cardiovascular conditions, or infectious diseases, offering stable and cost-effective alternatives to biological recognition elements.

In separation and purification (Solid-Phase Extraction – SPE), MIPs are exceptionally effective in SPE columns where their highly selective binding sites can be utilized to extract and purify specific compounds from complex mixtures, thus, particularly valuable in isolating trace components from pharmaceutical, environmental, or food samples, and they can also be precisely designed for challenging separations, such as the separation of enantiomers, crucial in drug development.[20,21] Accordingly, MIPs offer a powerful tool for isolating natural compounds from intricate botanical extracts, with their ability to selectively bind to target natural products, even when present in low concentrations within complex matrices, making them invaluable for the purification and extraction of bioactive compounds. Examples of which may include: the highly selective extraction of flavonoids, terpenoids and alkaloids from various plant sources, yielding high purity and recovery rates.

The ongoing evolution of MIP synthesis techniques and their integration into advanced analytical platforms continue to expand their utility, providing innovative solutions for complex challenges in research and industry. MIP production involves polymerizing functional monomer (*s*) and cross-linker (*s*) in the presence of the target molecule, known as the template. Upon removal of the template, the resulting polymeric matrix retains tailored cavities capable of selectively rebinding to the target molecule from a complex matrix, offering a powerful tool for the purification and extraction of natural products from complex extracts.[22,23]

Bulk polymerization is reported to be the most prevalent technique for the preparation of MIPs used for the extraction of natural products like quercetin from *Plectranthus scutellarioidesc*,[24] chicoric acid from chicory herb (*Cichorium intybus* L.),[25] sinipic acid from broccoli *(Botrytis italica* L.*)*,[26] chlorogenic acid from *Eucommia ulmoides* leaves,[27] and catharanthine from *Catharanthus roseu*.[28] These examples collectively demonstrate the enduring utility and effectiveness of bulk polymerization in producing MIPs for the selective and efficient isolation of a wide array of valuable natural products from diverse and complex plant sources.

Bulk polymerization involves the polymerization of a solution containing the template molecule (*T*), functional monomer(*s*) (FM), a cross-linking agent (CL), and a polymerization free radical initiator. The fundamental principle of this approach lies in the *in situ* generation of a polymeric network that spatially conforms around the template. Subsequent removal of the template molecule leaves behind a multitude of specific recognition sites within the polymer matrix, designed for selective rebinding. Although this technique is comparably the simplest and shows significant affinity and selectivity, it still has a few limitations, including shape irregularity and heterogeneous binding site distribution. Moreover, grinding and sieving processes could destroy some of the binding sites, loss of polymer yield, besides being time-consuming.[29,30]

Surface imprinting technology, leveraging silica prepared by the Stober process,[31] is emerging as a compelling alternative to mitigate the inherent limitations of bulk polymerization in MIP fabrication. This approach relies on the high mechanical and chemical stability, inertness, and non-swelling characteristics of silica particles. The core strategy for their synthesis involves the superficial localization of specific binding sites on a polymeric surface deposited on silica, thereby affording a significantly enhanced population of readily accessible recognition sites that exhibit remarkable specificity and selectivity for the targeted molecules compared to bulk polymerization.[32]

Recent examples of natural compounds isolated using surface imprinting polymerization included Various flavonoids that have been targeted using surface imprinting strategies like Rutin, Morin, Kaempferol, Naringin, Hesperidin, Luteolin, from different sources also resveratrol from *Polygonum cuspidatum* extract and purification of ginsenosides from ginseng, all of these compounds were isolated using surface imprinting method providing more accessible and homogeneous binding sites, leading to improved

selectivity, faster kinetics, and higher recovery rates for target compounds in complex natural matricies.[24,33–35]

The current study explores the use of molecularly imprinted polymers (MIPs), for the first time, as a selective and eco-friendly alternative for chemical, biological, and enzymatic extraction techniques of simmondsin from *Simmondsia chinensis* residual seeds. Based on computational design, Itaconic acid was selected as a functional monomer to be used in bulk and surface-imprinted MIPSs and comparatively tested for their ability to selectively isolate simmondsin from the complex extract. What is more significant is evaluating their impact on the protein content of the residual seeds, as a promising approach for extraction without reducing the nutritional content, which lowers the economic value of the residual seeds as a rich animal feed together with selective extraction of simmondsin to be further evaluated as an anti-obesity reagent.

2. Experimental

2.1 Reagents

Itaconic acid (ITC), ethylene glycol dimethacrylate (EGDMA), 2-2′-azoisobutyronitrile (AIBN), dimethylsulfoxide (DMSO), (3-aminopropyl) triethoxysilane (APTES), and ammonia solution 33%, were obtained from Sigma-Aldrich (Germany). Tetraethyl orthosilicate (TEOS) was purchased from Merck (Germany), Methanol (MOH) and Acetonitrile (ACN) HPLC grade were purchased from Supelco (Merck) (Germany), Triethylamine (TEA) was purchased from SDFCL (India), Simmondsin (SIMM) and Simmondsin acetate analytical standards were extracted and purified in Nawah Company (Egypt). Hyaluronic acid and glucose analytical standards were purchased from Sigma-Aldrich (Germany).

2.2 Equipment

All measurements were conducted using the HPLC system, Waters 2695 Separation Module (USA), connected to a Waters 996 Photodiode Array Detector,(USA), using a TOSOH TSKgel C18 column (250 × 4.6 mm, 5 μm particle size, (Japan) and Data acquisition and processing were performed using Empower 3 software. Protein content is measured by Buchi Kjeldahl, model K365, (Switzerland), pH adjustment using Hanna pH meter model Edge, (USA), orbit shaker (Stuart, UK) was used for incubating MIPs and NIPs with SIMM solutions during the rebinding experiments, vacuum evaporator -Buchi, model V100 (Switzerland), FTIR measurements were carried out at the Central Microanalysis Laboratory, Faculty of Science, Cairo University, using an FTIR-Affinity-1 (Japan from Shimadzu Corporation). Scanning Electron microscopy imaging was performed by QUANTA FEG250 (Netherlands) at the National Research Center (NRC), Giza, Egypt and Brunauer–Emmett–Teller (BET) Quanta Chrome Touch Win instruments (USA). Atomic Force Microscopy analysis (AFM), Agilent USA.

2.3 Synthesis of the polymers

2.3.1. Bulk polymerization. Molecularly imprinted polymers (MIPs) and their corresponding non-imprinted polymers (NIPs) were synthesized using a self-assembly approach. To optimize the polymer composition, four distinct cross-linker ratios (20%, 30%, 40%, and 50%) were investigated. Computational calculations using Gaussian 09 software determined the optimal template: monomer ratio of 1 : 4. The preparation process was performed by adding 1 mmol SIMM dissolved in the porogenic solvent (DMSO) in a screw-capped glass tube. Following, the functional monomer was added, and the pre-polymerization mixture was shaken for 30 min. Then, the cross-linker (EGDMA) was added, and the solution was allowed to mix for 2 min. To initiate polymerization, 0.913 mmol (150 mg) of free radical initiator (AIBN) were used, followed by purging with nitrogen for 2 min to remove any entrapped oxygen. Finally, the glass vial was sealed and placed in an oil bath at 60 °C for 24 hours, a schematic diagram for the synthesis is shown in Fig. 1(a).

The bulk polymer MIP (B) was then collected from the glass vials, crushed, ground, and sieved to obtain the desired particle size than The template was then extracted by subjecting the prepared polymers to a series of successive washings using a mixture of methanol/acetic acid (9 : 1, v/v), in which a total of 400 mL was employed, followed by a series of washings with 100% methanol, using a total of 200 mL. The extraction process was continued till the template was no longer detected in the filtrate using HPLC-PDA at 217 nm. Non-imprinted polymers were prepared using the same procedure as the MIPs, except for the absence of the template molecule. The NIPs (B) were also subjected to the same washing steps to ensure comparable properties.

2.3.2. Surface polymerization. This method is characterized by adding silica nanoparticles to increase the polymer surface area and enhance the surface-exposed recognition sites, which will reflect on better interaction with the template and reduction of non-specific binding that commonly occurs in bulk-based polymers.

The process started with the preparation of silica nanoparticles to be sued as a core based on Stöber's process[31] as follows: 120 mL of ethanol was stirred with 30 mL of 25% ammonia solution for 15 min at 500 rpm. Another 30 mL of ethanol was stirred with 6 mL of TEOS for 10 min. The two solvent mixtures were then mixed together and stirred for 35 min. The resulting mixture was then centrifuged at 3000 rpm for 15 min, followed by washing with ethanol, sonication for 30 min, and finally centrifugation at 3000 rpm. The silica nanoparticles were then dried in an oven at 50 °C under vacuum to be used for the imprinting step.

The surface imprinted polymers, MIPs (S), were synthesized by adding 300 mg of silica nanoparticles to 0.4 ml APTES, 200 ml DMSO in a quick fit conical flask (250 ml), and the mixture was sonicated for 30 min. Afterwards, 1 mmol of SIMM and 4 mmol of ITC were added as mentioned in the bulk polymerization process based on the computational results of the template: Functional monomer ratio, and the mixture was stirred for 30 minutes. Then, the cross-linker (EGDMA) was added at different ratios (20, 30, 40, and 50 mmol), and the solution was allowed to mix for 2 min. To initiate polymerization, 0.913 mmol (150 mg) of the free radical initiator (AIBN)

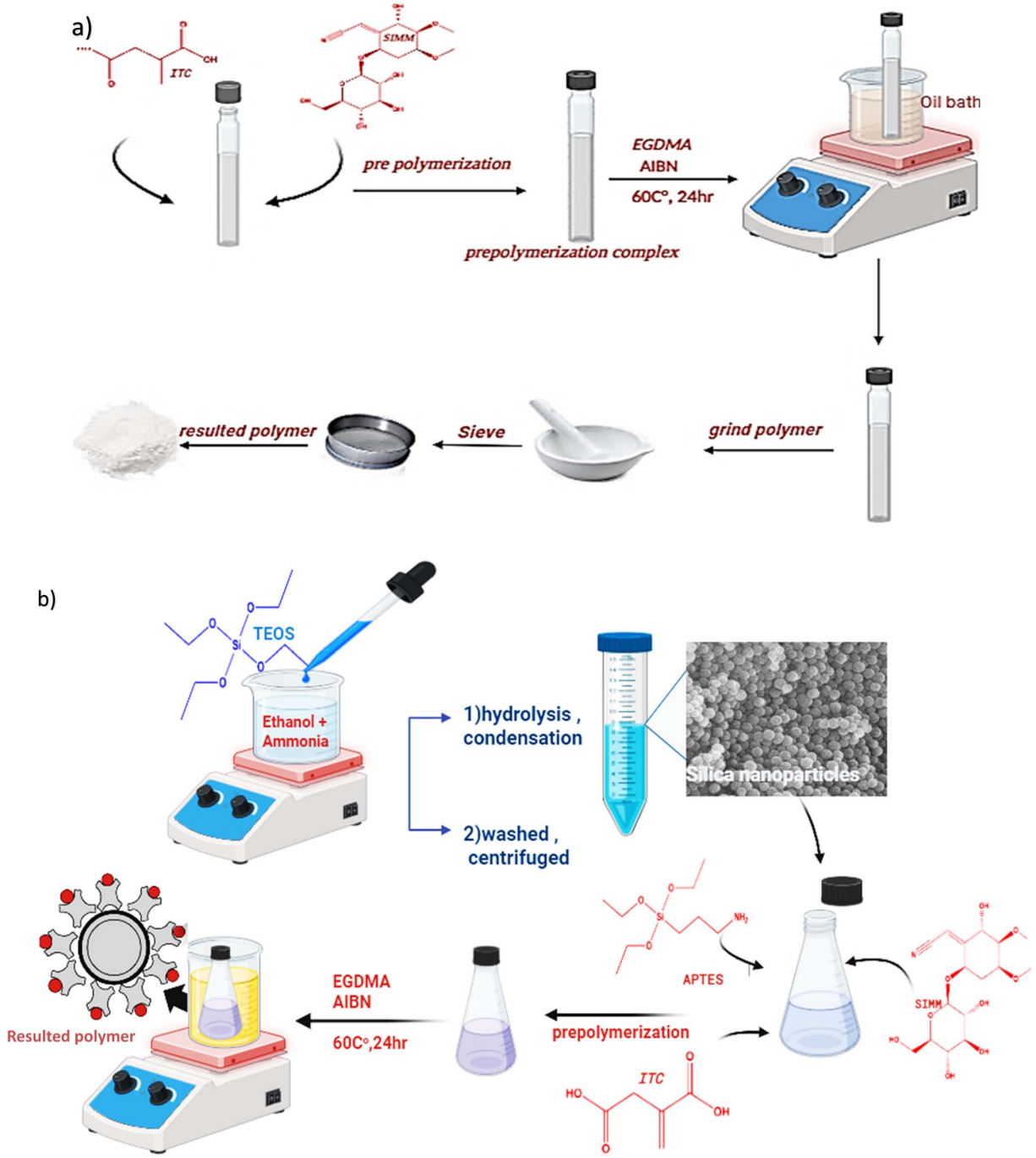

Fig. 1 Schematic diagram for (a) bulk and (b) surface polymerization method.

was added, followed by purging with nitrogen for 2 min. The glass conical flask was finally sealed well and placed in an oil bath at 60 °C for 24 hours as shown in Fig. 1(b). The resulting polymer was washed with acetone until free from DMSO. The fraction was finally collected without any need to crush or sieve, unlike the case of bulk polymerization, while the template was removed using the same washing procedures applied for bulk polymerization. Non-surface imprinted polymers (NIPS) were prepared using the same procedure as the MIPs, except for the absence of the template molecule. These NIPs were washed with the same method of surface-imprinted polymers to ensure that they have similar properties.

2.4 Equilibrium batch rebinding studies

The imprinting efficiency of the prepared polymers was determined by optimizing the best polymer in terms of incubation time, binding capacity, binding isotherm, and selectivity towards SIMM.

To evaluate the performance of various molecularly imprinted polymers (MIPs) and their corresponding non-imprinted

polymers (NIPs) for SIMM binding, 100 mg of each polymer was incubated with 5 mL of a 0.02 mM SIMM in methanol–water (50 : 50 v/v) at room temperature for 20 minutes. After centrifugation (10 000 rpm, 10 min) and filtration (0.22 μm PTFE syringe filter), the concentration of free SIMM in the supernatant was determined using high-performance liquid chromatography (HPLC).

A six-point calibration curve was constructed over the concentration range of 0.01–0.15 mM SIMM. The template rebinding capacity. The amount of the template rebound (B mmol g^{-1}) was calculated for each polymer using eqn (1)

$$B = \frac{(C_i - C_f) \times V \times 1000}{W} \quad (1)$$

where C_i and C_f are the initial and final concentration of the incubated solution, respectively, in mM, V is the volume of the solution in mL, and W is the weight of the polymer added in mg.

The imprinted factor was then calculated using eqn (2).

$$IF = \frac{q_{MIP}}{q_{NIP}} \quad (2)$$

To investigate the binding behavior of the selected MIP and corresponding NIP, binding isotherms were constructed by plotting the equilibrium binding capacity (B) against the initial simmondsin concentration (C_i). For each polymer, 100 mg of each surface polymer of bulk polymer were incubated with 5 mL of SIMM concentrations ranging from 0.07 to 0.4 mM for 20 minutes.

2.5 Structural and morphological characterization of the prepared polymers

Fourier-transform infrared spectroscopy (FTIR) and scanning electron microscopy (SEM) were utilized to characterize the chemical composition and physical morphology of the polymers. FTIR spectra were collected in the range of 500–4000 cm^{-1} to identify functional groups. SEM images provided a visual representation of the polymer surface. The Brunauer–Emmett–Teller (BET) method was employed to determine the surface area and pore volume of the polymers. Before analysis, the polymers were degassed for 24 hours to remove adsorbed gases and moisture. Nitrogen adsorption/desorption isotherms were then measured to calculate the surface area. Atomic Force Microscopy analysis (AFM) is a valuable characterization technique, providing nanoscale images of MIP surfaces. This allows for detailed analysis of their morphology, including pore size distribution (particularly relevant for surface-imprinted polymers) and surface roughness, which aids in understanding how the imprinting process influences the polymer's physical structure.

2.6 Selectivity

To assess the selectivity of the best MIP, its binding capacity for the template (simmondsin) was compared to that of structurally similar compounds. For each experiment, 100 mg of each surface and bulk polymer was incubated with various concentrations of 0.1 mg ml^{-1} prepared using (50% methanol : 50% water as diluent) of SIMM and different structurally related compounds s, like sucrose, hyaluronic acid, and simmondsin acetate with three different concentration 0.1, 0.5 and 1 mg ml^{-1} prepared with same diluent of SIMM, for 20 minutes. The amount of bound compounds was quantified using a six-point calibration curve constructed using the HPLC-PDA for SIMM n and SIMM acetate detection at 217 nm and hyaluronic acid at 205 nm, but the sucrose detection using an HPLC refractive index detector and water as mobile phase as following method of analysis.[36] This allowed for a direct comparison of the MIP's affinity for simmondsin and its analogs, providing valuable information about its selectivity.

2.7 HPLC/PDA measurements and method validation

All SIMM quantification measurements were done using HPLC-PDA detection and a mobile phase composed of 0.1% triethylamine (TEA) in water (A) and acetonitrile (ACN) (B), delivered in a gradient elution mode. Initially, the mobile phase composition was 87% A, maintained for 3 min, followed by a linear decrease to 80% A until 7 min, and subsequently to 40% A until 20 min. Column re-equilibration was performed from 20 to 25 min. The flow rate was 1 mL min^{-1}, at an injection volume of 10 μL. The HPLC-UV method was thoroughly validated to ensure reliability and accuracy, with validation parameters including linearity, limit of detection (LOD), limit of quantification (LOQ), intra-day precision, and inter-day precision.

2.8 Application of MIP to a real sample (*Simmondsia chinensis* residual seeds)

Residual jojoba seeds (100 g) were subjected to a three-step extraction process using 80% ethanol in a 1 : 4 ratios, each lasting for 24 hours. The resulting extract was concentrated to 20 g using a rotary vacuum evaporator at 40 °C, and then the dried residue was stored in an opaque glass jar.

To prepare the total extract solution, 200 mg of the extract were dissolved in 50 mL of a methanol–water mixture (50 : 50, v/v). The best molecularly imprinted polymer (MIP) was then equilibrated with 5 mL of this extract solution for 20 minutes. The reduction in SIMM content within the total extract was quantified using the same HPLC method previously described.

The protein analysis was performed using Kjeldahl analyzer to elucidate the impact of simmondsin extraction on the protein content before and after extraction using guidelines for the determination of nitrogen by the Kjeldahl method).[37] The procedure involved adding 10 g of a mixture of copper sulfate and potassium sulfate as a catalyst to the sample. Subsequently, 20 ml of concentrated sulfuric acid was added to the mixture. The digestion was then carried out in a speed digester at 400 °C for 1 hour. Following digestion, the sample, containing ammonium sulfate, underwent distillation and subsequent titration using the Kjeldahl Analyzer to determine the final protein content.

3. Results and discussion

3.1 Computational calculations for rational MIP design

Computational methods are being employed to streamline the design of high-affinity molecularly imprinted polymers (MIPs). By utilizing quantum mechanical simulations and statistical analyses, researchers can effectively predict the optimal functional monomer and template-to-monomer ratio, thereby reducing the reliance on traditional, time-consuming, and resource-intensive experimental methods. To achieve this, computational calculations were performed using Gaussian 09 software, applying density functional theory (DFT) at the B3LYP/6-31G(d) level. This approach enabled the calculation of binding energy (ΔE) between simmondsin and various functional monomers (Acrylamide (ACM), Itaconic acid (ICT), Methacrylic acid (MAA) and 4-vinyl pyridine (4-VP)).

The computational modelling involved two primary steps: structural optimization and template monomer model, in structural optimization the structures of each functional monomer and SIMM were individually optimized, and their corresponding energies were calculated, template: monomer ratio optimization, where a template-monomer model was constructed, followed by geometry optimization and binding energy calculation.

$$\Delta E = E(\text{template} - \text{monomer}) - E(\text{SIMM}) - E(\text{monomer}) \quad (3)$$

The effectiveness of a molecularly imprinted polymer (MIP) in recognizing its target molecule depends significantly on the strength and quantity of the interactions between the functional monomer and the template.[38] Therefore, optimizing the polymer composition is a critical step in MIP preparation.

Traditionally, selecting the appropriate functional monomer and determining its optimal molar ratio has been a time-consuming process. However, computational modeling has emerged as a valuable tool, significantly reducing the experimental time required for MIP development. By simulating the interactions between the functional monomer and the template, computational models can provide insights into the potential performance of different functional monomers and molar ratios, guiding experimental efforts towards more promising candidates, which accelerates the development of MIPs with desired recognition properties.[39,40]

In this study, the binding energy (E) between various monomers and SIMM was calculated using Gaussian software. Based on the results presented in Table 1, itaconic acid exhibited the highest E value −1851.417393 H compared to acrylamide, methacrylic acid, and 4-vinyl pyridine, that exhibited E values −1603.688703, −1662.856950 and −1682.078656, respectively, indicating that itaconic acid has superior binding affinity. Subsequently, rational design calculations were conducted to optimize the itaconic acid-to-simmondsin ratio in DMSO as the solvent phase using the same methodology, and the binding energy was calculated for different ratios, with the results summarized in Table 2.

While simmondsin has six potential binding sites, a 1 : 4 itaconic acid-to-simmondsin ratio was found to be optimal, as illustrated in Fig. 2. A ratio of 1 : 5 resulted in steric hindrance, leading to less favorable binding energy and geometry, and thus no further higher ratios were tested (Fig. 2).

Table 1 The calculated binding energies between SIMM and the different functional monomers[a]

Template to monomer	E (hartree)
SIMM-ACM	−1603.688703
SIMM-ITC	−1851.417393
SIMM-4-VP	−1682.078656
SIMM-MAA	−1662.856950

[a] 1 Hartree = 2625.5 kJ mol^{-1}.

Table 2 The calculated binding energies between SIMM and the best functional monomers

Molecule (in solvent phase)	E (hartree)	ΔE (hartree)	ΔE (kJ mol^{-1})
SIMM	−1356.400007	—	—
ITC	−495.044603	—	—
SIMM-(ITC)1	−1851.456372	−0.011762	−30.881131
SIMM-(ITC)2	−2346.515431	−0.014907	−39.138406
SIMM-(ITC)3	−2841.569575	−0.018052	−47.395598
SIMM-(ITC)4	−3336.626599	−0.021197	−55.652839

3.2 Evaluation of synthesized MIPs and corresponding NIPs

3.2.1. Equilibrium rebinding studies. Evaluating the efficiency of a Molecularly Imprinted Polymer (MIP) involves assessing its ability to selectively bind and recognize its target molecule. Firstly, the optimization of rebinding time, which refers to the time required for the MIP to rebind with the target analyte (simmondsin), is a crucial parameter in evaluating the performance of a MIP.[41]

In this study, 50 mg MIP (B) or MIP (S) were mixed with 5 ml of 0.02 mM of SIMM solution. The mixtures were mechanically shaken at 500 rpm for time intervals of 5–40 min, as shown in Fig. 3(a), then the amount of free SIMM in each time interval was estimated using HPLC. The optimum adsorption time was found to be 20 min, thus, was chosen as the optimum rebinding time for the adsorption properties measurements.

To estimate the quantity of MIPs or NIPs required to achieve maximum absorption needed for efficient rebinding, different amounts of each MIP (B), and MIP (S) and their corresponding NIPs ranging from 25 to 200 mg were added to 5 mL of a standard 0.02 mM of SIMM solution and the mixtures were mechanically shaken at 500 rpm for 20 min. Through a systematic investigation of varying polymer amounts, it was determined that the highest adsorption percentage and binding capacity for both MIP(B) and MIP(S) were consistently achieved when utilizing 100 mg of each polymer. Quantities lower than this optimal amount, specifically 25 mg and 50 mg, exhibited a proportionally reduced binding capacity, indicating an insufficient number of active sites to capture the target analytes

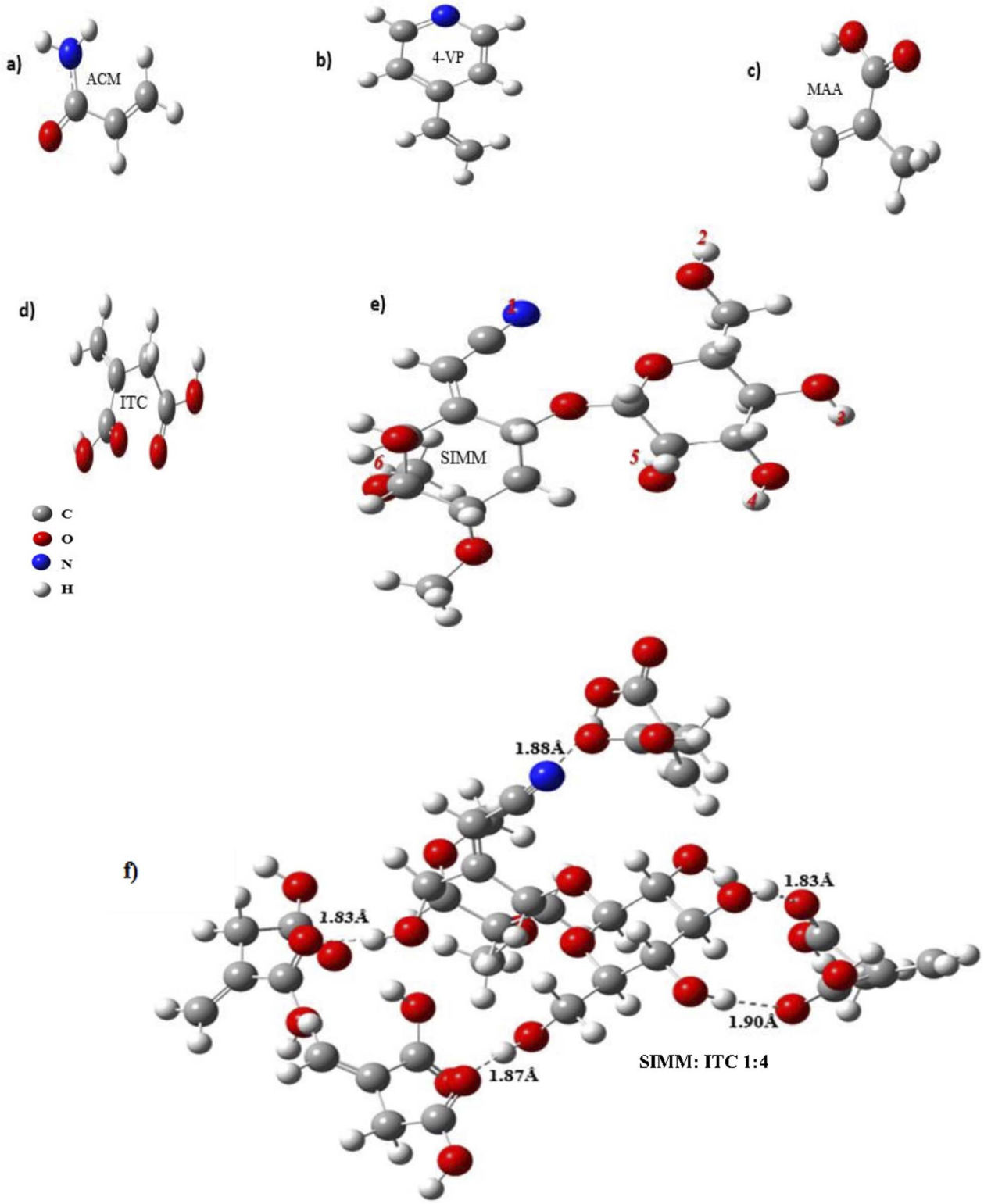

Fig. 2 The optimized monomer structures and simmondsin (a) is ACM, (b) is the 4-VP, (c)MAA, (d) ITC, (e) is the SIMM, and (f) is the optimized SIM : ITC (1 : 4), respectively.

effectively. Conversely, increasing the polymer amount beyond 100 mg, to 150 mg and 200 mg, did not yield a significant increase in binding capacity and the adsorption efficiency plateaued, suggesting that the available active sites were saturated and additional polymer offered no further advantage. Therefore, 100 mg were identified as the optimal polymer mass

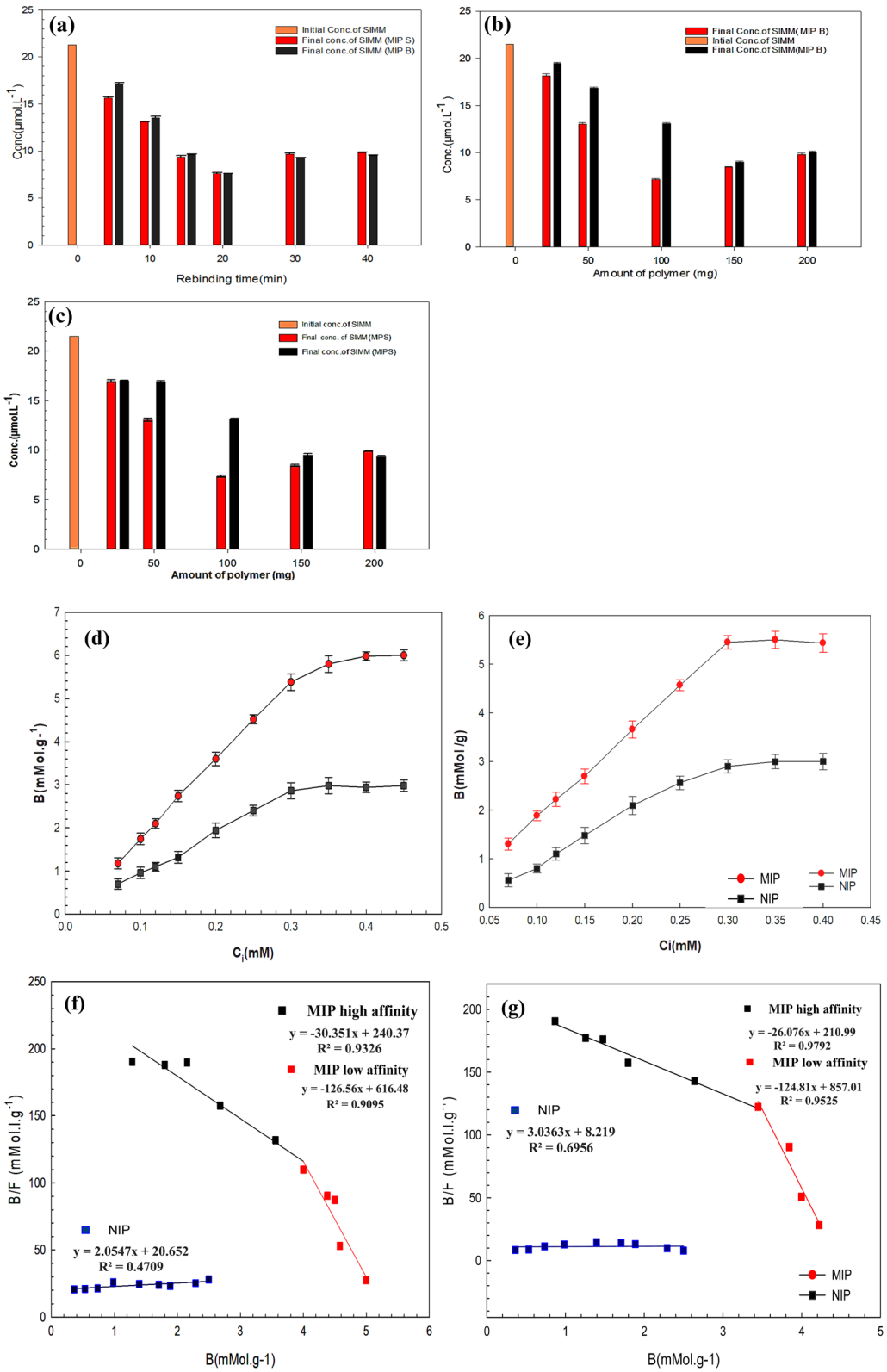

Fig. 3 (a) The effect of incubation time of MIP B, MIP S, (b) and (c) the effect of the amount of polymer used of MIP B, and MIP S, respectively, with corresponding NIP, (d) and (e) Binding isotherms of MIP B, MIP s and NIP for polymers with ratio (1 : 430), (1 : 4 : 40) respectively (f) and (g) Scatchard analysis of MIP B, MIP S and their corresponding NIP.

Table 3 Prepared polymeric ratios and their corresponding imprinting factor (IF)

	Template (mmol)	Functional monomer (mmol)	Crosslinker (mmol)	Imprinting factor (IF)
MIP (B)	1	4	20	1.02
NIP (B)	—	4	20	—
MIP (B)	**1**	**4**	**30**	**1.17**
NIP (B)	—	4	30	—
MIP (B)	1	4	40	1.01
NIP (B)	—	4	40	—
MIP (S)	1	4	30	1.05
NIP (S)	—	4	30	—
MIP (S)	**1**	**4**	**40**	**1.30**
NIP (S)	—	4	40	—
MIP (S)	1	4	50	0.95
NIP (S)	—	4	50	—

to attain the highest binding capacity, representing an efficient balance between resource consumption and adsorption performance, as visually corroborated by the data presented in Fig. 3(b) and (c).

To evaluate the impact of crosslinker ratio on MIP performance, MIP (B), and MIP (S) polymers at different crosslinker's ratios were incubated with 0.02 mM simmondsin solution for 20 min, as summarized in the results in Table 3. The findings of this step unequivocally demonstrated that the ratios of 1 : 4 : 30 for MIP (B) and 1 : 4 : 40 for MIP (S) yielded the most efficient simmondsin rebinding, evidenced by their highest imprinting factors (IFs) of 1.17 and 1.30, respectively. These ratios signify an optimal balance between creating stable recognition sites and maintaining polymer flexibility conducive to effective molecular capture.

Further increases in the crosslinker ratio beyond these optimal points were found to negatively impact binding efficiency. For instance, in MIP (S), increasing the crosslinker ratio from 1 : 4 : 40 to 1 : 4 : 50 resulted in a notable decrease in the IF to 0.95, significantly lower than the optimal 1.30. This reduction can be primarily attributable to excessive polymer rigidity, which can restrict the accessibility and flexibility of the imprinted cavities, thereby hindering efficient simmondsin rebinding. Similarly, decreasing the crosslinker ratio below the identified optimal values also proved detrimental.

For MIP (B), reducing the crosslinker ratio to 1 : 4 : 20 led to a lower IF of 1.02, compared to the optimal 1.17 for the 1 : 4 : 30 ratio. While for the MIP (S), a decrease to 1 : 4 : 30 resulted in an IF of 1.05, which is substantially lower than its optimal IF of 1.30 at the 1 : 4 : 40 ratio. Such decreases in IF at lower crosslinker concentrations likely stem from insufficient structural stability, potentially leading to poorly defined or collapsible recognition sites upon template removal. Therefore, the 1 : 4 : 30 ratio for MIP (B) and the 1 : 4 : 40 ratio for MIP (S) were conclusively identified as the optimal crosslinker ratios, maximizing simmondsin rebinding efficiency by providing a balance between sufficient structural integrity and appropriate cavity flexibility.[42]

3.2.2. Binding isotherm and scatchard analysis. Adsorption isotherm analysis, based on equilibrium binding data, was used to quantitatively characterize the interactions between the synthesized MIP and SIMM, allowing the evaluation of the efficiency of the imprinting process.[43] The homogeneity of binding sites was specifically assessed using the Langmuir isotherm model, by sketching the correlation between the initial incubated concentrations and the amount of bound template as shown in the binding isotherms given in Fig. 3(d) and (e) for bulk and surface polymers, respectively.

Analysis of the binding isotherms revealed a concentration-dependent adsorption profile for SIMM on both MIP (B) and MIP (S) variants, compared to their corresponding NIPs. At lower analyte concentrations (0.07–0.2 mM), marginal variations in binding capacities were observed across all polymers, suggesting a predominance of non-specific interactions. However, a significant divergence in binding behavior emerged within the higher concentration range (0.3–0.45 mM), characterized by a substantial increase in SIMM adsorption onto the MIP (B) and MIP (S) surfaces relative to the NIP controls. This variation indicates the manifestation of specific binding events, likely attributed to the presence of tailored recognition cavities within the MIP matrices, in addition to the inherent surface adsorption observed in all polymers.

The observed binding patterns aligned closely with the Langmuir adsorption isotherm model, which indicates a homogeneous distribution of binding sites across the MIP surface and a monolayer adsorption mechanism devoid of lateral interactions.[25,44] This conformity suggests that the imprinting process successfully generated a uniform population of high-affinity binding sites, facilitating selective analyte capture. Furthermore, the observed saturation behavior at higher concentrations supports the Langmuir model's assumption of a finite number of binding sites, reinforcing the efficacy of the molecular imprinting strategy in creating materials with predictable and controlled binding properties.[45]

Furthermore, the rebinding data of MIP (B), MIP (S) and their corresponding NIPs were processed using Scatchard analysis as shown in Fig. 3(f) and (g), in which the ratio of bound to free template (B/F) was plotted as a function of the amount of bound SIMM (B). This analysis effectively reveals the presence of heterogeneous binding sites, which The Scatchard

analysis is based on the following general equation $\left(\frac{B}{F}\right) = \left(\frac{B_{max} - B}{K_d}\right)$.[46]

Where B is the binding capacity of the polymer in mmol g^{-1}, F is the final free simmondsin concentration, B_{max} is the maximum number of binding sites, and K_d is the equilibrium dissociation constat, B_{max} as well as K_d were determined for both the areas of high and low affinities. B_{max} was calculated by dividing the y intercept by the slope of the equation, while the K_d is the reciprocal of the slope each characterized by a distinct dissociation constant (K_d) and maximum binding capacity (B_{max}).

A lower K_d value signifies higher binding affinity, indicating stronger interaction with the target molecule, while a higher B_{max} denotes a greater number of available binding sites.[47,48]

The Scatchard plots and derived parameters for MIP (B)and MIP (S) demonstrate the impact of synthesis methodology on binding characteristics. A two intersecting straight lines plot was attained, indicating the heterogeneous binding nature of the MIP (B) and MIP (S) binding sites for the tested concentrations, for MIP (B),MIP (S) the concentration range of (0.07–0.25 mM) that represents the high affinity binding sites and the other range of (0.25–0.45 mM) represents the low affinity binding sites.

The adsorption capacities B_{max} were calculated as shown in Fig. 3(f) and (g) which has two linear equations in high and low affinity which the $B_{max} = \frac{y - \text{intercept}}{-\text{slope}}$ and, $K_d \frac{1}{-\text{slope}}$[49] based on the previous general equation, the resulting B_{max} was depicted to be 7.920 and 9.110 mmol g^{-1} with dissociation constants K_d 0.0329 and 0.424 for MIP (B) and MIP (S), respectively at high affinity binding sites and.

While at low affinity sites, the adsorption capacities B_{max} were 5.0831and 6.865 mmol g^{-1} with dissociation constants K_d 0.0082 and 0.008 for MIP (B) and MIP (S), respectively. Also, the consistent presence of these high-affinity (low K_d) sites in both MIP types, in contrast with the non-specific, low-capacity binding of the NIP, confirms the successful imprinting process.

The variation in K_d and B_{max} between MIP (B) and MIP (S) highlights how different synthesis routes can selectively influence the accessibility, quantity, and quality of specific binding sites, thereby fine-tuning the material's overall binding performance for various applications.[47]

While the experimental data for the Non-Imprinted Polymer (NIP), suggests that over the range of tested simmondsin concentrations, NIPs exhibited a limited adsorption capacity that is nearly constant across the experimental setup, irrespective of whether the sample was prepared *via* NIP (B) or NIP (S), accordingly, the adsorption capacity did not significantly vary with a increasing the initial concentration of simmondsin.

3.3 Characterization of polymers

3.3.1. Fourier transform infrared. The FTIR spectra of SIMM, unwashed and washed MIP (B), MIP (S), and their corresponding NIPs were acquired in the 4000–500 cm^{-1} range. The washed MIPs and NIPs exhibited similar FTIR spectra, suggesting that both polymers possess a comparable backbone structure as shown in Fig. S1.

SIMM displays characteristic absorption bands at approximately ~3400 cm^{-1} (O–H stretching vibration), 2970 cm^{-1} (C–H stretching vibration), 2260 cm^{-1} (C≡N stretching vibration), ~1650 cm^{-1} (C=C stretching vibration), and ~1060 cm^{-1} (C–O stretching vibration). The bulk polymers showed similarities in their FTIR spectra; peaks at ~2970 cm^{-1} corresponded to (C–H stretching vibrations), while characteristic peaks at ~1625, ~1710 cm^{-1}, and ~3400 cm^{-1} represented (C=C, C=O, and O–H stretching vibrations), respectively. These results confirm that the bulk polymers have a similar backbone, with poly (ITC) and poly (EGDMA) molecules present within the polymer matrix.

For surface imprinted polymers, three peaks were observed in all spectra at~527 and ~955 cm^{-1}, represented (Si–O–Si and Si–OH stretching vibrations), and a peak at 1050 cm^{-1} represented (Si–O–Si asymmetric stretching), at ~3400 cm^{-1} represented (O–H stretching vibration) these peaks are correlated to the silica nanoparticles. This similarity in FTIR spectra between washed MIPs and NIPs supports the successful extraction of SIMM during the washing procedure.

3.3.2. Scanning electron microscopy analysis. Scanning Electron Microscopy (SEM), is commonly employed to visualize particles across a range of sizes and to characterize the diverse geometrical structures of MIPs. In addition to determining particle size and morphology, SEM analysis has demonstrated the potential of differentiating between MIPs and their corresponding (NIPs) for bulk and surface imprinting polymers.[50]

The surface morphology of both bulk and surface-washed MIPs shown in Fig. 3(A)b and f displays distinct porous sites, not observed in the corresponding NIPs. This observation suggests that the MIPs possess a higher density of adsorption sites, potentially leading to enhanced adsorption capacity for the target compound. Bulk polymer particles have exhibited a size ranging from 5 to 50 micrometers, with an irregular morphology when observed at a magnification of 5000×.

In contrast, silica nanoparticles displayed a monodisperse, spherical shape with an average diameter of 144 ± 10.4 nanometers, as observed at a magnification of 30000×. The deposited coatings on the silica nanoparticles were relatively thin, resulting in a slight decrease in the particle size for both MIP (S) and NIP (S) compared to the bulk particles. The average particle size of the MIP and NIP-coated silica was determined to be 120.5 ± 12.3 nanometers.

3.3.3. Atomic force microscopy analysis. Atomic Force Microscopy (AFM), is a powerful technique for characterizing molecularly Imprinted Polymers (MIPs) and their corresponding non-imprinting polymers (NIPs), providing valuable insights into their structural and morphological features. AFM provides high-resolution images of MIP surfaces, allowing for direct visualization of the imprinted cavities or binding sites created during the polymerization process.[51,52]

As shown in Figure 4(B), AFM 3D images for unwashed, washed MIP B and its corresponding NIP B surfaces (a), (b), and (C), respectively, and (d), (e), and (f) for unwashed, washed MIP S and its corresponding NIP S modified polymers. It can be

observed from the images that the NIP film was relatively more uniform and flatter than washed MIP. The observed higher surface roughness in both washed MIP B, MIP S were 7.96, 13.14 nm, respectively which can be attributed to the creation of cavities within the polymer matrix.

These cavities increase the overall surface area and introduce significant surface irregularities, leading to an elevated roughness value (RMS). Interestingly, the unwashed MIP B, MIP S exhibited a higher roughness value compared to the corresponding NIP B, NIP S, which were 7.52, 10.69, 6.16 and

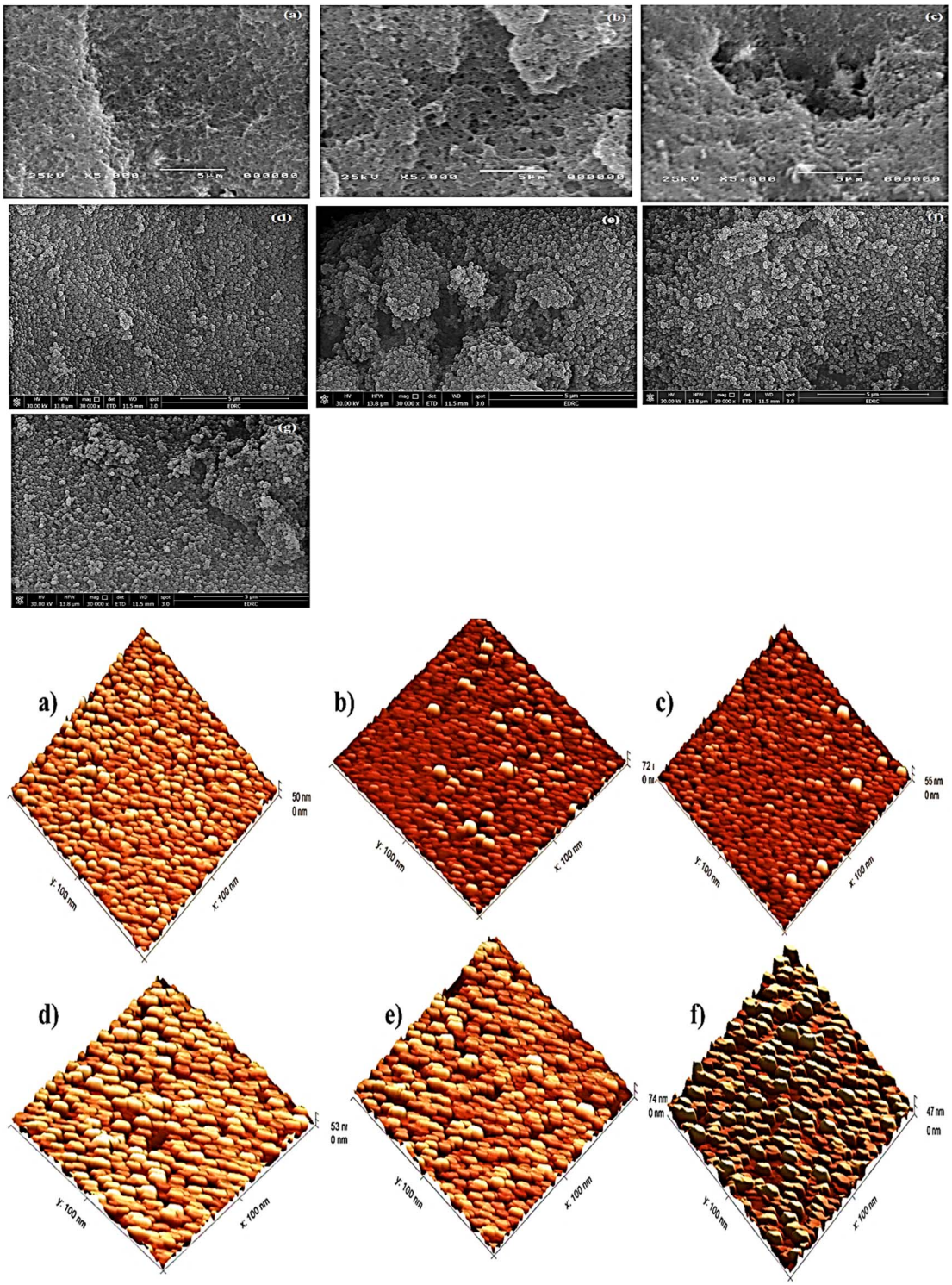

Fig. 4 (A): SEM images of (a) MIP (B) unwashed, (b) MIP (B) washed, (c) NIP (B), (d) bare silica, (e) MIP (S) washed, (f) MIP (S) unwashed, and (g) NIP (S). (B): AFM 3D images for (a) unwashed MIP (B), (b) washed MIP (B), (c) NIP (B), (d) unwashed MIP (S), (e) washed MIP (S),and (f) NIP (S).

8.59 nm, respectively. This observation can be attributed to the presence of the SIMM template within the polymeric film. The embedded template may interfere with polymer chain growth during polymerization, potentially leading to a more irregular and rough surface compared to the washed MIP where the template has been removed.[53]

The higher roughness observed in MIP (S) compared to MIP (B) can be attributed to several factors, including the presence of silica nanoparticles, increased surface area, heterogeneous polymer growth, and potential aggregation of silica nanoparticles.

3.3.4. Bett-Teller (BET) and Barrett–Joyner–Halenda (BJH) analysis. Molecular imprinting processes are known to induce significant alterations in the polymeric matrix, resulting in the formation of a multitude of pores, cavities, and other structural defects. N_2 adsorption/desorption measurements were used to determine the Brunauer–Emmett–Teller (BET) for surface area and Barrett–Joyner–Halenda (BJH) to indicate the pore diameter and pore volume of the washed and unwashed MIP (B) and MIP (S) and their corresponding NIPs as given in Table 4.[54,55]

A comparative analysis was conducted on the textural properties of bulk-polymerized MIP (MIP B) and surface-imprinted MIP (MIP S), along with their non-imprinted polymer (NIP) counterparts and, for MIP S and the uncoated silica support.

For MIP B, the results reveal a higher surface area for the washed polymer (69.64 $m^2 g^{-1}$) compared to its corresponding NIP B (58.9 $m^2 g^{-1}$). This increase in surface area upon template removal strongly indicates the successful creation of imprinted cavities within the polymer matrix. Interestingly, the unwashed MIP B exhibited the lowest surface area (51.45 $m^2 g^{-1}$), suggesting that the presence of the template molecules initially occupies a significant portion of the internal surface. Despite these variations in surface area, both washed and unwashed MIP B, as well as NIP B, displayed comparable pore volumes. However, the washed MIP B possessed a slightly higher pore volume than its NIP counterpart, despite exhibiting a similar average pore diameter. This subtle yet significant difference points towards the formation of mesopores (pores with diameters $\geq$2 nm) within the washed MIP B, which are crucial for enhancing analyte accessibility.

A consistent pattern was observed for the surface-imprinted polymer (MIP S) where the washed MIP S showed a higher surface area (78.34 $m^2 g^{-1}$) compared to its corresponding NIP S (58.9 $m^2 g^{-1}$) and even the uncoated silica support (95.76 $m^2 g^{-1}$). The reduction in surface area from uncoated silica to the NIP and then to the MIP (though MIP S is still higher than NIP S) suggests successful polymer coating on the silica surface. Importantly, the washed and unwashed MIP S, along with their corresponding NIP S and the coated silica, displayed comparable pore volumes and pore diameters.

Critically, the measured pore diameters were consistently less than 2 nm, unequivocally indicating the predominant formation of nanopores (or micropores, pore diameter <2 nm) within the surface-imprinted structure. Such nanopores are highly advantageous as they are reported to provide well-defined recognition sites and a large accessible surface area, facilitating precise interaction with the target molecule[56]

On comparing the two synthesis approaches, the MIP S exhibited a notably higher surface area (78.34 $m^2 g^{-1}$) compared to MIP B (69.64 $m^2 g^{-1}$). This higher surface area in MIP S is indicative of a greater number of accessible pores and cavities. This structural advantage directly contributes to an increased binding capacity for modified MIPs, as a larger surface area with superficially exposed specific recognition sites which provides more opportunities for interaction with the target analyte. Overall, these findings underscore the profound impact of synthesis methodology and template removal on the final porous characteristics and, consequently, the adsorption performance of MIPs for natural product isolation.

3.4 Competitive selectivity study

A critical parameter for evaluating the efficacy of Molecularly Imprinted Polymers (MIPs) is their selectivity, which determines their ability to discriminate between the target analyte and structurally similar compounds. This discriminatory power is not merely a desirable trait, but rather a fundamental requirement for the practical application of MIPs across diverse fields.[57]

In this study to evaluate the MIPs' selectivity, we measured solutions containing a fixed concentration of SIMM (0.1 mg ml^{-1}) in the presence of varying concentrations of structurally analogous molecules such as sucrose, hyaluronic acid, and simmondsin acetate at an equal concentrations of simmondsin and 5, 10 times higher concentration which, 100 mg from each MIP (B), MIP (S) and there corresponding NIPs added to each mixture and the recovery percent resulted are summarized in Table 5. The obtained data compellingly illustrates the significant selectivity of both MIP (B) and MIP (S) for simmondsin.

Quantitatively, the removal efficiency for SIMM reached 81.01% $\pm$ 0.10. For MIP (B) and (92.46% $\pm$ 0.02) for MIP (S). In stark contrast, the removal percentages for the structurally similar interferents did not exceed 20%, indicating a minimal degree of non-specific binding and confirming the successful imprinting of recognition sites specific to SIMM.

Table 4 Surface area, pore volume, and pore size of polymers using BET and BJH methods

	Unwashed MIP (B)	Washed MIP (B)	NIP (B)	Uncoated silica	Un washed MIP (S)	Washed MIP (S)	NIP (S)
BET surface area ($m^2 g^{-1}$)	51.45	69.64	58.96	95.76	68.50	78.34	72.45
BJH pore volume(cc g^{-1})	0.06	0.09	0.07	0.13	0.17	0.10	0.24
BJH pore diameter(nm)	2.65	1.95	2.31	1.42	1.99	1.74	1.88

3.5 HPLC method validation

The applied HPLC-UV method underwent rigorous validation following the International Conference on Harmonization (ICH) guidelines, encompassing a comprehensive evaluation of linearity, limit of detection (LOD), limit of quantification (LOQ), precision (both intra-day and inter-day), and accuracy.

Linearity was established by serially diluting a stock standard simmondsin solution (1 mg mL^{-1}) to yield six distinct concentrations ranging from 0.05 to 0.8 mg mL^{-1}. Each concentration was injected in triplicate into the HPLC system, and the resulting calibration curve, generated by plotting observed peak areas *versus* corresponding concentrations as shown in Fig. S2, demonstrated excellent linearity with a squared regression coefficient (R^2) of 0.9998. The calculated LOD (3.3 σ/S) and LOQ (10 σ/S), derived from the calibration curve parameters, where "σ" is the standard deviation of the intercept and S is the slope of the calibration curve, were found to be 0.0015 mg mL^{-1} and 0.00428 mg mL^{-1}, respectively.

Precision was assessed through the evaluation of intra-day and inter-day variation using multiple injections of a 0.2 mg mL^{-1} standard solution. Intra-day repeatability, determined from replicate injections within a single day, exhibited a low relative standard deviation (% RSD) of 0.85% while inter-day intermediate precision, assessed through multiple injections of the same standard solution on different days, also demonstrated good reproducibility with a calculated %RSD of 0.78%.

Accuracy was evaluated using a recovery experiment based on a 0.4 mg mL^{-1} extract spiked with three different amounts of the SIMM standard. The analysis of the unspoked extract and spiked samples, performed in triplicate, yielded recovery percentages calculated as follows equation.

$$\text{Recovery} = \frac{\text{Amount of SIM in spiked extract} - \text{Amount of SIM in extract before spiking}}{\text{Spiked amount}} \times 100$$

These values ranged from 99.00% ± 1.76–102.13% ± 0.66, collectively, these validation parameters confirm that the developed HPLC-UV method exhibits good linearity, sensitivity, accuracy, and precision, rendering it suitable for its intended analytical application and evaluation of MIPs efficiency.

4. Analytical applications

4.1 Application of MIP (B),(S) to the real sample of jojoba seeds total extract

Jojoba meal, a protein-rich byproduct generated after oil extraction from *Simmondsia chinensis* seeds, presents a significant nutritional advantage as a potential protein source. However, its utilization has been considerably hampered by the presence of the toxic cyanogenic glycoside and simmondsin. This inherent toxicity has compelled researchers to actively pursue and investigate alternative methodologies aimed at the effective detoxification of jojoba meal, thereby unlocking its valuable protein content for broader applications(Ahmed, Mohamed, and Abu-Salem 2023; Feki *et al.* 2022).[58,59]

The present investigation established a foundational, facile, expeditious, and convenient molecularly imprinted polymer (MIP) methodology, employing both bulk and surface imprinting strategies, for the direct extraction of simmondsin from a complex *Simmondsia chinensis* residual seed extract.

To evaluate the binding kinetics, 100 mg aliquots of MIP (B) and MIP (S) were equilibrated with 5 mL of the total simmondsin extract for a 20-minute incubation period. High-performance liquid chromatography (HPLC) chromatograms of the total extract solution, obtained before and following the incubation with the MIPs, are presented in Fig. 5(A) and (B). The chromatographic profile of the crude simmondsin extract revealed four major constituents, with simmondsin peak (c) and simmondsin 2-ferulate peak (d) identified at retention times (RT) of 4.7 and 13.8 minutes, respectively.

As depicted in Fig. 5(A) and (B), a significant attenuation in the peak area corresponding to simmondsin was observed post-incubation with both MIP variants, in contrast to the relatively

Table 5 Removal % of simmondsin and some of its structural analogies at different conc 0.1, 0.5 and 1 mg ml^{-1})

Analyte	MIP (B) (R %)	MIP (S) (R %)	NIP (B) (R %)	NIP (S) (R %)
Simmondsin	81.01% ± 0.10	92.46% ± 0.02	21.55 ± 0.15	23.31 ± 0.3
Simmondsin acetate (1×)	13.66 ± 1.68	17.66 ± 1.02	14.03 ± 0.70	12.96 ± 1.30
Simmondsin acetate (5×)	14.72 ± 1.24	16.57 ± 0.36	12.96 ± 1.60	13.52 ± 1.43
Simmondsin acetate (10×)	11.51 ± 0.81	13.68 ± 1.27	11.78 ± 1.10	11.53 ± 0.61
Sucrose (1×)	16.071 ± 0.93	13.154 ± 1.09	16.4256 ± 1.35	16.275 ± 0.50
Sucrose (5×)	13.93 ± 1.39	17.35 ± 0.55	13.57 ± 1.10	15.37 ± 0.85
Sucrose (10×)	11.33 ± 1.73	12.36 ± 1.50	11.51 ± 1.32	11.32 ± 1.89
Hyaluronic acid (1×)	19.17 ± 1.05	21.05 ± 0.21	15.67 ± 1.66	16.22 ± 1.60
Hyaluronic acid (5×)	18.26 ± 0.93	22.08 ± 1.21	15.35 ± 1.08	13.69 ± 1.32
Hyaluronic acid (10×)	21.55 ± 1.96	20.62 ± 1.77	15.92 ± 0.93	18.48 ± 0.73

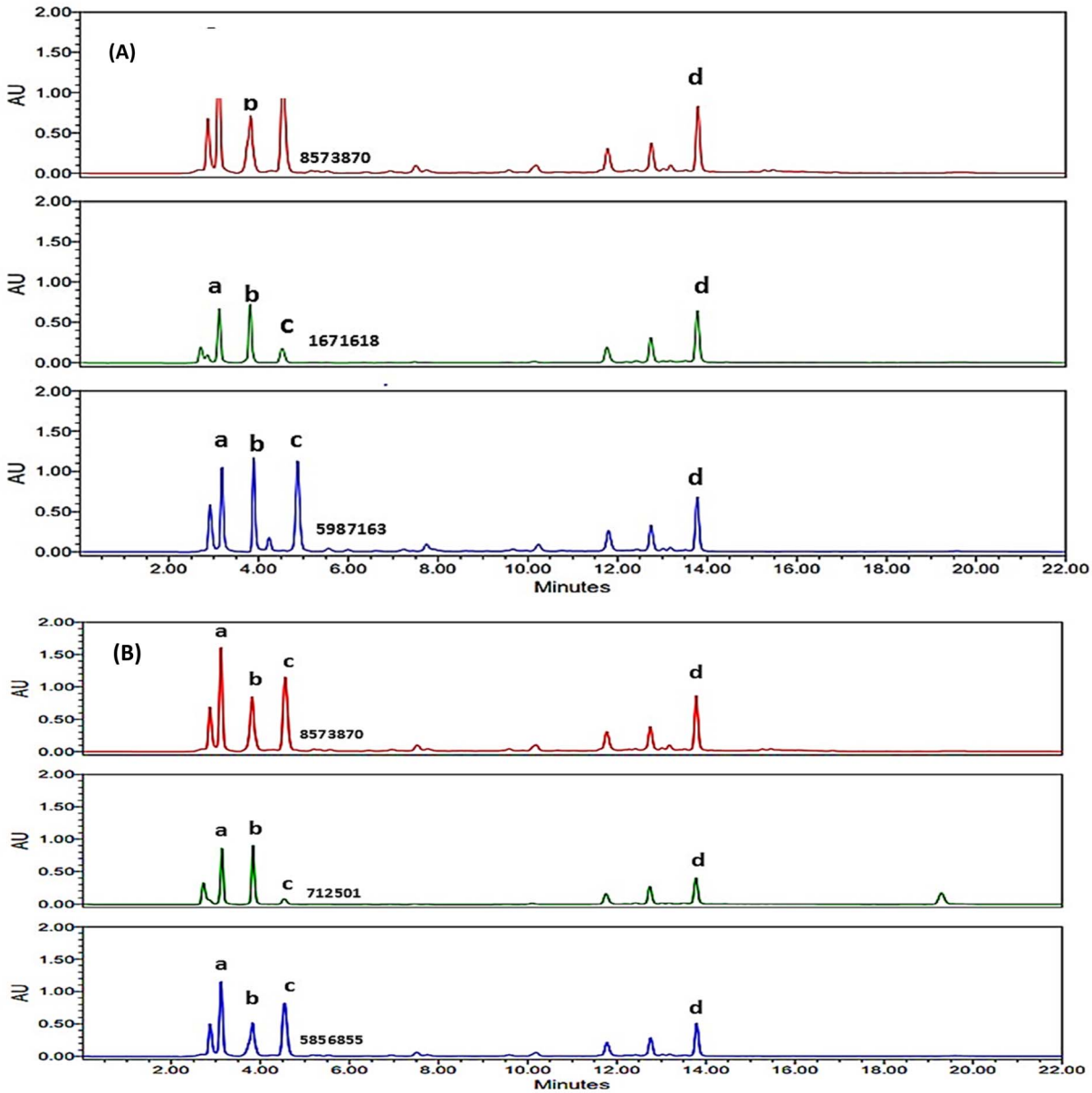

Fig. 5 (A) and (B) are Chromatograms of simmondsin total extract solutions before and after incubation with MIP, NIP (B) and MIP, NIP (S), respectively. (a, and b) are compounds present in the total extract that were not identified in this study, (c) is the simmondsin and (d) is 2-simmondsin ferulate.

unchanged peak intensities of the other co-extracted compounds. Quantitative analysis of simmondsin removal efficiency indicated that the surface-imprinted polymer, MIP (S), exhibited superior performance (92.46% ± 0.02) compared to conventional extraction techniques, while the bulk-imprinted polymer, MIP (B), achieved a removal rate of 81.01% ± 0.10. These findings assure the potential of surface-imprinted polymers for the selective and efficient extraction of simmondsin directly from complex plant matrices.

Also, the molecularly imprinted polymers, MIP (B) and MIP (S) exhibited a noteworthy ability to remove the undesirable compound simmondsin 2-ferulate from the jojoba meal matrix. Quantifiable reductions of 14.95 ± 1.24% and 19.15 ± 1.22% were achieved by MIP (B) and MIP (S), respectively. This removal is considered a positive outcome as simmondsin 2-ferulate is an unwanted component that can potentially impact the quality or downstream processing of jojoba-derived products. However, while any level of reduction of this specific compound is beneficial, its overall effect is less substantial when compared to the removal of the primary target, simmondsin.[60,61]

This can be largely attributed to the fact that the concentration of simmondsin 2-ferulate in the raw jojoba meal is approximately half that of simmondsin, thus limiting the overall impact of its removal on the total composition. Systematically comparing and highlighting methods for the removal of SIMM, solvent extraction methods stand out for their

high simmondsin removal efficiencies. Organic solvents like methanol and ethanol demonstrate showed even higher efficacy, frequently reaching 99% simmondsin removal yet carries significant drawbacks, as many of such solvents are hazardous and flammable, posing safety risks and requiring stringent handling protocols.

Beyond solvent extraction, biological approaches such as microbial and enzymatic methods have also shown promising results, achieving high percentages of simmondsin removal by degrading the compound. Despite their high efficiency and potential for specificity, these methods face considerable limitations that restrict their widespread application. A primary drawback is their high cost, as enzymes and specific microbial cultures can be expensive to produce and purify on an industrial scale. Additionally, both microbial and enzymatic processes are often highly sensitive to operational conditions like pH and temperature, making process control complex and reducing their overall robustness and reusability in industrial scale.[3,7]

A significant factor contributing to the widespread application and economic viability of Molecularly Imprinted Polymers (MIPs) is their remarkable reusability. This characteristic allows MIPs to be regenerated and reused multiple times, making them a cost-effective and sustainable alternative to single-use materials. Both MIP S and MIP B, when used to bind the target compound SIMM, can be effectively regenerated. This process typically involves washing the MIP with a specific solvent mixture, in this case, a 1 : 1 water : methanol solution. This mixture effectively disrupts the interactions between SIMM and the imprinted binding sites within the polymer, allowing for the removal of approximately 95% of the bound compound. To ensure the MIP is thoroughly clean and ready for its next binding cycle, an additional wash with 100% methanol is then performed.

The effectiveness of this regeneration protocol is evident in the high removal efficiency observed, with a reported recovery efficiency of 96.461% ± 1.02% for MIP (S) and 93.713 ± 0.791% for MIP (B) of the bound SIMM. This high recovery rate is crucial for maintaining the MIP's binding capacity and selectivity over multiple uses. In this particular instance, the MIPs were successfully reused for five consecutive rebind/regeneration cycles while maintaining their excellent rebinding efficiency.

4.2 Protein recovery from *Simmondsia chinensis* residual (jojoba meal)

Jojoba meal is a notable source of protein, present in high concentrations, making it a potentially valuable protein supplement, especially in regions where conventional feed sources are scarce or expensive.[62,63] In addition to the protein content, some studies have indicated the presence of beneficial compounds like phytic acid and polyphenols, which possess antioxidant properties.

The primary focus of the current study is to develop a cost-effective and scalable method to remove SIMM in jojoba meals without significantly degrading its protein content and nutritional value. The initial protein content of jojoba meal, was quantified using a Kjeldahl Analyzer. Subsequently, the extraction process was implemented and the resultant total extract was subjected to treatment with molecularly imprinted polymers (MIPs) to selectively remove the simmondsin compounds. Following this detoxification step, the processed, simmondsin-depleted extract was reintroduced and thoroughly spiked into the original jojoba meal. Finally, a comprehensive analysis of the protein content in this reconstituted material was performed and compared to the content present in the initial jojoba meal.

The initial jojoba meal, before treatment, had a protein content of 33.01% ± 1.20%, while the reconstituted meal after treatment had a protein content of 25.88% ± 0.72%, % which is comparable to the estimated range of 26–33% before extraction. This represents a favorable outcome, considering the high simmondsin removal rate of 92.46% ± 0.02 achieved by the MIP (S) technique.

In comparison, solvent extraction with 80% ethanol, shown in other studies to be effective in removing 94.66% of simmondsin,[64] resulted in a lower protein content of 13.33% ± 0.62. Other solvent extraction methods using methanol, isopropanol, and acetone resulted in higher protein contents of 29.10% ± 3.6%, 28.82% ± 3.33%, and 29.20% ± 4.10%, respectively, but exhibited lower simmondsin removal percentages.[7]

Alternative methods, such as microwave and microbiological treatments, have demonstrated good results in achieving high simmondsin removal while preserving high protein content, but they are often time-consuming and cost-prohibitive at an industrial scale.[3,15]

Comparative analysis of the results of the current study and those of previously established methodologies reveals a notable advantage of the present approach, primarily attributed to its efficacy in preserving the inherent protein content of the jojoba meal. Furthermore, when considered within the framework of sustainable practices, this method distinguishes itself as a greener alternative, characterized by lower consumable usage and demonstrably effective simmondsin removal. The capacity to maintain protein integrity while minimizing resource consumption underscores the superior profile of this MIP-based extraction strategy compared to conventional techniques.

5. Conclusion

In summary, this study establishes a robust foundation for a simple, rapid, and convenient method employing bulk and surface-imprinted polymers for the selective extraction of SIM from the complex matrix of *Simmondsia Chinensis* residual seed extract. The surface-imprinted polymers MIP (S) demonstrated superior performance compared to conventional extraction methods, achieving a simmondsin removal rate of 92.46% ± 0.02, and kept 25.88% ± 0.72% of protein content in jojoba meal, which is comparable to the estimated range of 26.0–33.0% before extraction, while the bulk-imprinted polymers MIP (B)removed 81.01% ± 0.1.

The incorporation of silica nanoparticles contributed to a substantial increase in the exposed surface-active binding sites, thereby enhancing the removal efficiency and selectivity of

MIP (S). Following optimization, the developed highly selective polymer matrices exhibited excellent potential for removing simmondsin, a primary toxic compound in jojoba seed residue, while preserving a high protein ratio, crucial for potential downstream applications of the residual seed extract. This newly developed extraction method presents several significant advantages over conventional techniques. Specifically, it is more environmentally friendly, cost-effective, and aligns with sustainable concepts, offering promising potential for scale-up to industrial batch extractions. Furthermore, the enhanced selectivity of the MIP (S), attributed to the increased active sites from nanoparticle incorporation, represents a significant advancement in extraction methodologies for complex plant matrices, potentially reducing the need for extensive purification steps. Thus, this work can be considered as a promising approach for simmondsin extraction without reducing the nutritional content, which lowers the economic value of the residual seeds as a rich animal feed together with selective extraction of simmondsin to be further evaluated pharmacologically as an anti-obesity reagent and standardizing the efficient dose for its application.

Conflicts of interest

The authors have no competing interests to declare that are relevant to the content of this article. The authors declare receiving no fund for the current manuscript.

Data availability

All data are included within the manuscript and supplementary information (SI). Supplementary information is available. See DOI: https://doi.org/10.1039/d5ra08130k.

References

1 M. Ozturk and K. R. Hakeem, *Plant and Human Health, Volume 2: Phytochemistry and Molecular Aspects*, Springer, 2019.
2 F. Feki, *et al.*, Optimization of microwave assisted extraction of simmondsins and polyphenols from Jojoba (Simmondsia chinensis) seed cake using Box-Behnken statistical design, *Food Chem.*, 2021, **356**, 129670.
3 F. Feki, *et al.*, Optimization of microwave assisted extraction of simmondsins and polyphenols from Jojoba (Simmondsia chinensis) seed cake using Box-Behnken statistical design, *Food Chem.*, 2021, **356**, 129670.
4 D. Arya and S. Khan, A review of Simmondsia chinensis (Jojoba) "the desert gold": A multipurpose oil seed crop for industrial uses, *J. Pharm. Sci. Res.*, 2016, **8**(6), 381.
5 A. A. Abd El-Rahman, I. M. Abd El-Aleem, A. E. El-Deeb, and A. E. Hussein, *Elimination of Toxic Compounds and Nutritional Evaluation of Jojoba Meal Proteins*, Benha Univ., 2006.
6 M. M. Cokelaere, H. D. Dangreau, S. Arnouts, E. R. Kuhn and E. M. P. Decuypere, Influence of pure simmondsin on the food intake in rats, *J. Agric. Food Chem.*, 1992, **40**(10), 1839–1842.
7 R. M. Elsanhoty, A. Al-Soqeer and M. F. Ramadan, Effect of detoxification methods on the quality and safety of jojoba (Simmondsia chinensis) meal, *J. Food Biochem.*, 2017, **41**(5), e12400.
8 D. M. El-Saidy, A. M. H. Abou Ashour, M. K. Abou EL-Naga and M. M. Abd-EL-Maksoud, Evaluation of jojoba seed meal (simmondsia chinensis) as partial and total replacement of fishmeal in nile tilapia, oreochromis niloticus (l.), fingerlings diets, *Menoufia J. Anim. Poult. Fish Prod.*, 2017, **1**(3), 27–40.
9 C. N. Boozer and A. J. Herron, Simmondsin for weight loss in rats, *Int. J. Obes.*, 2006, **30**(7), 1143–1148.
10 C. A. Y. González and A. J. Y. Soler, The natural compound dimethylsimmondsin present in jojoba reveals food restricting properties, *Food Funct. Food Sci. Obes.*, 2023, **1**(5), 1–6.
11 J.-S. Baek, *et al.*, Acarviosine-simmondsin, a novel compound obtained from acarviosine-glucose and simmondsin by Thermus maltogenic amylase and its *in vivo* effect on food intake and hyperglycemia, *Biosci., Biotechnol., Biochem.*, 2003, **67**(3), 532–539.
12 A. d'Oosterlynck, *Method for Separating the Toxic Resinous Fraction from Prepared Whole Jojoba Seeds or Jojoba Seed Press-Cake*, Sep-1997.
13 A. J. Verbiscar, *et al.*, Detoxification of jojoba meal, *J. Agric. Food Chem.*, 1980, **28**(3), 571–578.
14 T. P. Abbott, R. A. Holser, B. J. Plattner, R. D. Plattner and H. C. Purcell, Pilot-scale isolation of simmondsin and related jojoba constituents, *Ind. Crops Prod.*, 1999, **10**(1), 65–72.
15 T. P. Abbott, L. K. Nakamura, T. C. Nelsen, H. J. Gasdorf, G. A. Bennett and R. Kleiman, Microorganisms for degrading simmondsin and related cyanogenic toxins in jojoba, *Appl. Microbiol. Biotechnol.*, 1990, **34**, 270–273.
16 A. Bouali, A. Bellirou, N. Boukhatem, A. Hamal and B. Bouammali, Enzymatic detoxification of jojoba meal and effect of the resulting meal on food intake in rats, *Nat. Prod. Res.*, 2008, **22**(7), 638–647.
17 D. A. Gkika, *et al.*, Application of molecularly imprinted polymers (MIPs) as environmental separation tools, *RSC Appl. Polym.*, 2024, **2**(2), 127–148.
18 A.-M. Gavrilă, M. Ioni□ă and G. Toader, Recent Advances in Molecularly Imprinted Polymers and Emerging Polymeric Technologies for Hazardous Compounds, *Polymers*, 2025, **17**(8), 1092.
19 F. Hilaluddin, *et al.*, Recent applications of molecularly imprinted polymer sensors equipped with smartphones for detection of pesticide residues in environmental samples, *Arab J. basic appl. sci.*, 2024, **31**(1), 481–504.
20 L. Wang, M. Pagett and W. Zhang, Molecularly imprinted polymer (MIP) based electrochemical sensors and their recent advances in health applications, *Sens. Actuators Rep.*, 2023, **5**, 100153.
21 T. Hu, R. Chen, Q. Wang, C. He and S. Liu, Recent advances and applications of molecularly imprinted polymers in solid-

phase extraction for real sample analysis, *J. Sep. Sci.*, 2021, **44**(1), 274–309.
22 M. D. Ariani, A. Zuhrotun, P. Manesiotis and A. N. Hasanah, Magnetic Molecularly Imprinted Polymers: An Update on Their Use in the Separation of Active Compounds from Natural Products, *Polymers*, 2022, **14**(7), 1389.
23 G. Vasapollo, R. Del Sole, L. Mergola, M. R. Lazzoi, A. Scardino, S. Scorrano and G. Mele, Molecularly Imprinted Polymers: Present and Future Prospective, *Int. J. Mol. Sci.*, 2011, **12**(9), 5908–5945.
24 W. Li, A. Liang, Z. Lu and Y. Xie, Application of Molecular Imprinting Technique in Separation and Detection of Natural Products, *Eng. Proc.*, 2023, **49**(1), 1.
25 E. M. Saad, A. Madbouly, N. Ayoub and R. Mohamed El Nashar, Preparation and application of molecularly imprinted polymer for isolation of chicoric acid from Chicorium intybus L. medicinal plant, *Anal. Chim. Acta*, 2015, **877**, 80–89.
26 H. Hosny, N. El Gohary, E. Saad, H. Handoussa and R. M. El Nashar, Isolation of sinapic acid from broccoli using molecularly imprinted polymers, *J. Sep. Sci.*, 2018, **41**(5), 1164–1172.
27 E. Sieniawska and K. Skalicka-Woźniak, Isolation of chlorogenic acid from Mutellina purpurea L. herb using high-performance counter-current chromatography, *Nat. Prod. Res.*, 2014, **28**(21), 1936–1939.
28 C. Lopez, B. Claude, P. Morin, J.-P. Max, R. Pena and J.-P. Ribet, Synthesis and study of a molecularly imprinted polymer for the specific extraction of indole alkaloids from Catharanthus roseus extracts, *Anal. Chim. Acta*, 2011, **683**(2), 198–205.
29 D.-L. Huang, *et al.*, Application of molecularly imprinted polymers in wastewater treatment: a review, *Environ. Sci. Pollut. Res.*, 2015, **22**, 963–977.
30 A. M. Chrzanowska, A. Poliwoda and P. P. Wieczorek, Characterization of particle morphology of biochanin A molecularly imprinted polymers and their properties as a potential sorbent for solid-phase extraction, *Mater. Sci. Eng., C*, 2015, **49**, 793–798.
31 W. Stöber, A. Fink and E. Bohn, Controlled growth of monodisperse silica spheres in the micron size range, *J. Colloid Interface Sci.*, 1968, **26**(1), 62–69.
32 A. M. Chrzanowska, A. Poliwoda and P. P. Wieczorek, Surface molecularly imprinted silica for selective solid-phase extraction of biochanin A, daidzein and genistein from urine samples, *J. Chromatogr. A*, 2015, **1392**, 1–9.
33 R.-Z. Cao, *et al.*, A novel surface molecularly imprinted polymer based on the natural biological macromolecule sporopollenin for the specific and efficient adsorption of resveratrol from Polygonum cuspidatum extracts, *Int. J. Biol. Macromol.*, 2024, **280**, 136168.
34 Y. Zhang, *et al.*, Applications of molecular imprinting technology in the study of traditional Chinese medicine, *Molecules*, 2022, **28**(1), 301.
35 Y. Yang and X. Shen, Preparation and application of molecularly imprinted polymers for flavonoids: Review and perspective, *Molecules*, 2022, **27**(21), 7355.
36 A. A. F. Zielinski, C. M. Braga, I. M. Demiate, F. L. Beltrame, A. Nogueira and G. Wosiacki, Development and optimization of a HPLC-RI method for the determination of major sugars in apple juice and evaluation of the effect of the ripening stage, *Food Sci. Technol.*, 2014, **34**, 38–43.
37 J. M. Lynch and D. M. Barbano, Kjeldahl nitrogen analysis as a reference method for protein determination in dairy products, *J. AOAC Int.*, 1999, **82**(6), 1389–1398.
38 A. N. Hasanah, N. Safitri, A. Zulfa, N. Neli and D. Rahayu, Factors affecting preparation of molecularly imprinted polymer and methods on finding template-monomer interaction as the key of selective properties of the materials, *Molecules*, 2021, **26**(18), 5612.
39 I. A. Nicholls, K. Golker, G. D. Olsson, S. Suriyanarayanan and J. G. Wiklander, The use of computational methods for the development of molecularly imprinted polymers, *Polymers*, 2021, **13**(17), 2841.
40 M. Marć, T. Kupka, P. P. Wieczorek and J. Namieśnik, Computational modeling of molecularly imprinted polymers as a green approach to the development of novel analytical sorbents, *TrAC, Trends Anal. Chem.*, 2018, **98**, 64–78.
41 A. Doostmohammadi, *et al.*, Molecularly imprinted polymer (MIP) based core-shell microspheres for bacteria isolation, *Polymer*, 2022, **251**, 124917.
42 N. T. Abdel Ghani, R. Mohamed El Nashar, F. M. Abdel-Haleem and A. Madbouly, Computational Design, Synthesis and Application of a New Selective Molecularly Imprinted Polymer for Electrochemical Detection, *Electroanalysis*, 2016, **28**(7), 1530–1538.
43 N. F. Che Lah, A. L. Ahmad, S. C. Low and N. D. Zaulkiflee, Isotherm and electrochemical properties of atrazine sensing using PVC/MIP: Effect of porogenic solvent concentration ratio, *Membranes*, 2021, **11**(9), 657.
44 R. J. Umpleby, S. C. Baxter, A. M. Rampey, G. T. Rushton, Y. Chen, and K. D. Shimizu, *Characterization of the Heterogeneous Binding Site Affinity Distributions in Molecularly Imprinted Polymers*, 2004, vol. 804, pp. 141–149.
45 X. Ma, *et al.*, Magnetic molecularly imprinted polymers doped with graphene oxide for the selective recognition and extraction of four flavonoids from Rhododendron species, *J. Chromatogr. A*, 2019, **1598**, 39–48.
46 H. Bai, G. Teng, C. Zhang, J. Yang, W. Yang and F. Tian, Magnetic materials as adsorbents for the pre-concentration and separation of active ingredients from herbal medicine, *J. Sep. Sci.*, 2024, **47**(14), 2400274.
47 R. J. Ansell, Characterization of the binding properties of molecularly imprinted polymers, *Mol. imprinted Polym. Biotechnol.*, 2015, 51–93.
48 D. A. Spivak, Optimization, evaluation, and characterization of molecularly imprinted polymers, *Adv. Drug Delivery Rev.*, 2005, **57**(12), 1779–1794.
49 E. M. Saad, A. Madbouly, N. Ayoub and R. M. El Nashar, Preparation and application of molecularly imprinted polymer for isolation of chicoric acid from Chicorium intybus L. medicinal plant, *Anal. Chim. Acta*, 2015, **877**, 80–89.

50 G. De Middeleer, P. Dubruel and S. De Saeger, Characterization of MIP and MIP functionalized surfaces: Current state-of-the-art, *TrAC, Trends Anal. Chem.*, 2016, **76**, 71–85.
51 K. Navakul, C. Sangma, P. Yenchitsomanus, S. Chunta and P. A. Lieberzeit, Enhancing sensitivity of QCM for dengue type 1 virus detection using graphene-based polymer composites, *Anal. Bioanal. Chem.*, 2021, **413**, 6191–6198.
52 P. Nguyen-Tri, P. Ghassemi, P. Carriere, S. Nanda, A. A. Assadi and D. D. Nguyen, Recent applications of advanced atomic force microscopy in polymer science: A review, *Polymers*, 2020, **12**(5), 1142.
53 G. Siciliano, *et al.*, Development of an MIP based electrochemical sensor for TGF-β1 detection and its application in liquid biopsy, *Analyst*, 2023, **148**(18), 4447–4455.
54 M. G. Metwally, O. R. Shehab, H. Ibrahim and R. M. El Nashar, Electrochemical detection of Bisphenol A in plastic bottled drinking waters and soft drinks based on molecularly imprinted polymer, *J. Environ. Chem. Eng.*, 2022, **10**(3), 107699.
55 Z. Lin, *et al.*, Synthesis of uniformly sized molecularly imprinted polymer-coated silica nanoparticles for selective recognition and enrichment of lysozyme, *J. Mater. Chem.*, 2012, **22**(34), 17914–17922.
56 R. Tabaraki and N. Sadeghinejad, Preparation and application of magnetic molecularly imprinted polymers for rutin determination in green tea, *Chem. Pap.*, 2020, **74**(6), 1937–1944.
57 L. Wang, W. Fu, Y. Shen, H. Tan and H. Xu, Molecularly imprinted polymers for selective extraction of Oblongifolin C from Garcinia yunnanensis Hu, *Molecules*, 2017, **22**(4), 508.
58 D. M. M. Ahmed, R. K. Mohamed and F. M. Abu-Salem, Detoxification of Jojoba Meal Simmondsin by Production of Its Protein Isolates as a Protein Source in Food Applications, *Int. J. Halal Res.*, 2023, **5**(2), 58–71.
59 F. Feki, *et al.*, A jojoba (Simmondsia chinensis) seed cake extracts express hepatoprotective activity against paracetamol-induced toxicity in rats, *Biomed. Pharmacother.*, 2022, **153**, 113371.
60 N. S. Abu-Foul, N. J. Khudelr and S. D. Rofael, DETOXIFICATION OF JOJOBA (Simmondsia chinensis) MEAL WITH WATER, *J. Food Dairy Sci.*, 2004, **29**(4), 1927–1937.
61 A. Benzioni, D. Mills, M. Van Boven and M. Cokelaere, Effect of genotype and environment on the concentration of simmondsin and its derivatives in jojoba seeds and foliage, *Ind. Crops Prod.*, 2005, **21**(2), 241–249.
62 S. N. El Gendy, A. K. Elmotayam, R. Samir, M. I. Ezzat and A. M. El Sayed, A review of the desert gold jojoba (Simmondsia chinensis) whole plant, oil, and meal: Phytochemical composition, medicinal uses, and detoxification, *J. Am. Oil Chem. Soc.*, 2023, **100**(8), 591–614.
63 M. K. Shrestha, I. Peri, P. Smirnoff, Y. Birk and A. Golan-Goldhirsh, Jojoba seed meal proteins associated with proteolytic and protease inhibitory activities, *J. Agric. Food Chem.*, 2002, **50**(20), 5670–5675.
64 R. A. Holser and T. P. Abbott, Extraction of simmondsins from defatted jojoba meal using aqueous ethanol, *Ind. Crops Prod.*, 1999, **10**(1), 41–46.